Journal of Structural Geology, Vol. 13, No. 4, pp. 385 to 398, 1991
Printed in Great Britain

0191-8141/91 $03.00 + 0.00

Syn-diagenetic evolution of shear structures in superficial nappes: an example from the Northern Apennines (NW Italy)

P. LABAUME, C. BERTY and PH. LAURENT

Laboratoire de Tectonique (u.a. CNRS No. 1371), Université Montpellier II, Sciences et Techniques du Languedoc, 34095 Montpellier Cédex 5, France

(*Received* 23 *January* 1990; *accepted in revised form* 17 *August* 1990)

Abstract—In the superficial nappes of the Northern Apennines, meso- and microstructures in sheared mudstones and fine-grained turbidites consist mainly of networks of striated faults and calcite vein arrays. The striated faults correspond to the first generation of structures. They form two sets, respectively, synthetic and antithetic to the general shearing. Locally, a sigmoidal microfabric is associated with the synthetic faults in scaly deformation bands up to a few metres thick. Late laterally extensive calcite veins are superposed on these structures. They result from the opening of multiple releasing oversteps between shear surfaces. The 'crack–seal' mechanism of deformation played a major role in their formation. Structures of the first generation result from heterogeneous ductile deformation of initially poorly lithified and water-rich sediments. The late formation of the calcite veins corresponds to a transitional ductile–brittle behaviour in sufficiently lithified sediment. Evolution of structures probably depended on a strain-hardening process and was dependent on the progressive compaction and dewatering of the sediment. The gently dipping faults and veins probably formed the main pathway for the interstitial fluids, possibly overpressured, expelled from the sediment. We emphasize that the geometry of the structures described provides important shear-sense criteria for the study of superficial nappe tectonics.

INTRODUCTION

DURING the last decade, geophysical surveys and deep-sea drilling have shown that tectonic movements in the high structural levels of modern accretionary prisms occur mainly along low-angle shear zones displaying scaly fabrics and stratal disruption (e.g. Moore *et al.* 1982, 1986, Cowan *et al.* 1984, Behrmann *et al.* 1988, Agar *et al.* 1989). Similar shear zones have also been described in emerged ancient prisms and thrust-belts (e.g. Koopman 1983, Fisher & Byrne 1987, Platt *et al.* 1988, Agar *et al.* 1989, Lash 1989). In many cases, mineralized veins occur associated with these shear zones (e.g. Koopman 1983, Cloos 1984, Fisher & Byrne 1987, Behrmann *et al.* 1988, Platt *et al.* 1988, Vrolijk *et al.* 1988). They are usually thought to indicate high-pressure pore-fluid circulation in the shear zones. This interpretation is in accord with *in situ* measurements of pore-fluid overpressures in modern prisms (Moore *et al.* 1982, Von Huene 1985) and with evidence that shear zones act as preferential drains for escape of these fluids (Moore *et al.* 1988, Moore 1989, Henry *et al.* 1989).

However, in spite of these numerous studies, many problems regarding shear zone geometry and evolution remain. In particular, few studies deal with the structural patterns at the outcrop scale, although these are likely to give useful information on the deformation processes and shear-sense criteria. The kinematics of mineralized vein opening and the place and significance of these veins in the timing of the shear zone evolution are also rarely discussed in detail. In the case of drill-core studies, these limitations mainly result from 'spot-sampling' and the small scale of observations. Therefore, onland studies of ancient shear zones should provide a better understanding of shear deformation in accretionary prisms.

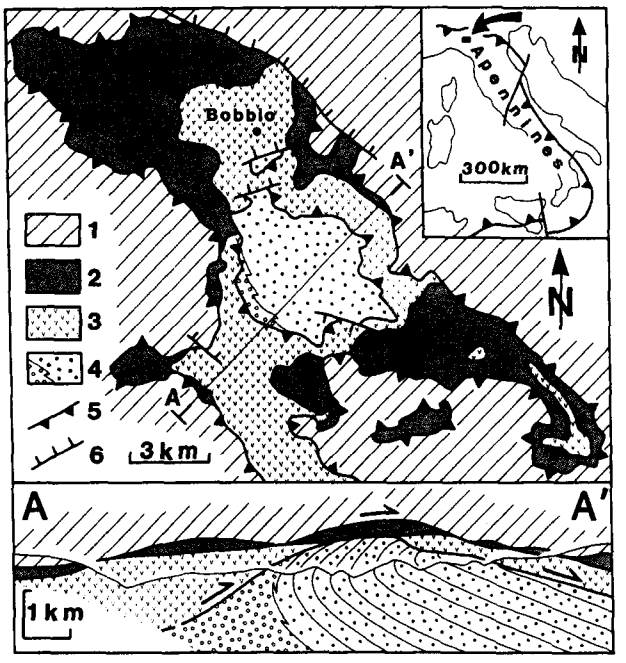

Fig. 1. General structure of the northern part of the Bobbio window (top: structural map, unpublished mapping by P. Labaume; bottom: section; inset: location). (1) Ligurian Units (Cretaceous turbidites and breccia); (2) Canetolo Unit (Paleocene–Eocene turbidites); (3) Coli Unit (elements of the Canetolo Unit featuring Oligocene–Early Miocene slope sediment apron); (4) lower unit (dots: Early Miocene foredeep turbidites of the Bobbio Formation; open circles: Early Miocene chaotic deposits of the foredeep inner border); (5) allochthonous unit contacts; (6) late normal faults.

In the present paper, we address these questions from shear structures of the Northern Apennines submarine superficial nappes. The structures studied occur in the Oligo-Miocene mudstones and turbidites of the 'Bobbio window', 60 km NE of Genova, NW Italy (Fig. 1, inset). Specific meso- and microstructure patterns and common

laterally extensive synkinematic calcite veins display a wide diversity of structures, the geometry, kinematics and chronology of which have been analysed. Dynamic data have been obtained from calcite twinning analysis in the veins. We discuss the evolution of deformation mechanisms during progressive nappe emplacement and we emphasize the potential use of these structures as shear-sense criteria.

GEOLOGICAL SETTING

The Northern Apennines are formed of stacked allochthonous units ('nappes') emplaced toward the northeast from the Oligocene to the Recent (e.g. Abbate *et al.* 1970, Elter 1973), during the convergence between the Europe and Apulia plates (Boccaletti *et al.* 1971, Kligfield 1979). Most of the outcropping units belong to the high structural levels. Until the Late Miocene, these superficial units were emplaced in submarine conditions, with syntectonic marine sedimentation taking place in the NW–SE-trending foredeep at their front (Umbro–Tuscan turbidite successions) (Ricci Lucchi 1986) and in piggy-back basins at their top (Ricci Lucchi 1987). The Northern Apennines thus form a wedge, the general evolution of which presents many analogies with oceanic accretionary prisms (Treves 1984), although they probably developed on continental crust from at least the Late Oligocene.

The northern part of the 'Bobbio window' (Fig. 1) shows the superposition of several of these superficial units (Bellinzona *et al.* 1968, Plesi 1974, Labaume *et al.* 1990a) as follows, from top to bottom. (1) The Ligurian Units are composed of Cretaceous turbidites and ophiolite-bearing breccia. (2) The Canetolo Unit is a sub-Ligurian unit made of Paleocene to Middle Eocene turbidites. (3) The Coli Unit comprises Paleocene–Eocene turbidites overlain by Oligocene to Early Miocene slope mudstones and thin-bedded turbidites (Labaume *et al.* 1990a). The slope mudstones contain common debris-flow deposit intercalations derived from the Paleocene–Eocene substrate. This succession represents an element of the Canetolo Unit covered by its Oligo-Miocene slope sediment apron. It is subdivided into numerous tectonic sub-units forming a complex duplex structure below the Canetolo Unit *sensu stricto*. (4) A lower unit is mainly composed of an Early Miocene turbidite succession, the Bobbio Formation (Mutti & Ghibaudo 1972), which represents an element of the Umbro–Tuscan foredeep infill (Ricchi Lucchi 1986). To the south, the Bobbio Formation onlaps chaotic slope deposits analogous to those of the Coli Unit. These deposits represent the chaotic base of slope apron formed at the front of the Canetolo Unit during its emplacement. The turbidites form a large recumbent syncline with a NE-vergence. This syncline is truncated by the sole thrust of the Coli Unit. Tectono-sedimentary relationships indicate that the chaotic deposits formed the southern border of the foredeep, and that this border migrated northward during the turbidite deposition, in response to slope progradation and to active compressive tectonics at the foredeep border (Reutter & Schlüter 1968, Mutti & Ghibaudo 1972, Labaume *et al.* 1990a). Eventually, this tectonics resulted in the northeastward thrusting of the allochthonous units onto the foredeep succession.

The Coli and Canetolo Units both show a lenticular geometry, their thickness varying laterally from several hundreds of metres to zero over a few kilometres in the direction of tectonic transport (Fig. 1). This indicates that a stage of low-angle extensional deformation followed the initial thrusting stage of these units. This extensional deformation may have resulted from gravitational collapse of the thrust units (Platt 1986). The nappe pile was later deformed by an antiformal folding probably related with an underlying thrust. Eventually, it was segmented by steep-dipping normal faults striking both parallel and transversely to the belt.

SHEAR DEFORMATION GEOMETRY AND KINEMATICS

Nappe emplacement is responsible for a complex shear deformation throughout the superposed units. In this paper, we deal only with those structures which occur in the Oligo-Miocene mudstones and turbidites of the Coli and lower units. These deposits form relatively massive bodies which display specific meso- and microstructure patterns more adapted to geometric and kinematic analysis than complex structures found in associated clay-rich bodies. Moreover, they are the youngest deposits of the area, and thus they have undergone only the most recent and well-known stages of nappe tectonics.

Sh–Sh′ *fault networks*

At the outcrop, the shear deformation is essentially characterized by a network of striated faults ranging from the cm to the 10 m scale. In this network, the major faults may bound rock lenses of different lithologies, being thus locally responsible for tectonic melange fabric (Fig. 2). Inside these lenses, the minor faults have a spacing of a few mm to dm and isolate apparently undeformed elements of rock, thus giving a more or less intense scaly fabric and/or stratal disruption (Fig. 3).

At all scales, the faults form two sets that have, respectively, gentle and steep dips. These sets are named *Sh* and *Sh′* (*Sh* for 'shear', Figs. 2 and 3), after Koopmann (1983) and Labaume *et al.* (1990b).

The low-angle *Sh* faults show a high degree of lateral continuity, and can be followed for several metres. They have a curviplanar shape and can splay and join, locally forming an anastomosed network. The *Sh′* faults dip steeply toward the SW, their average angle with the *Sh* faults usually varying from 50° to 70°. Individual *Sh′* faults usually show less lateral continuity than the *Sh* ones, but they are commonly closer spaced. Unlike the *Sh* faults, they do not form an anastomosing network

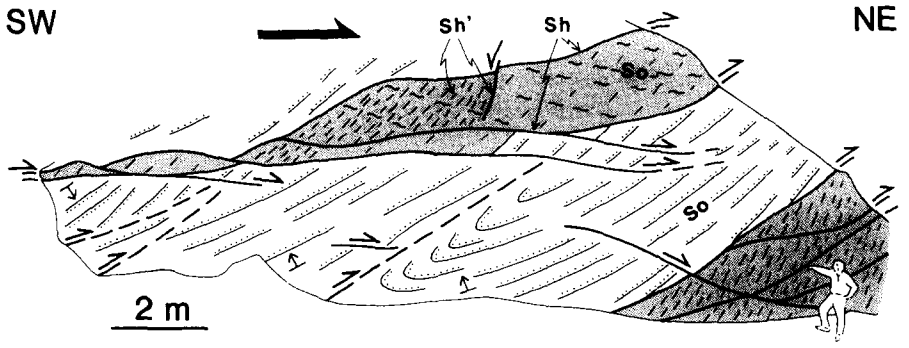

Fig. 2. Fault network in the Coli Unit, resulting from shearing toward the northeast and responsible for the tectonic melange fabric (structural position of outcrop: inset Fig. 3). Sediments are Oligocene mudstones (in grey) and turbidites (in white). Note that shearing is after the folding and thrusting in the turbidites. *Sh* and *Sh'*, respectively, synthetic and antithetic faults with respect to the general shearing; S_0, bedding (arrows point toward the stratigraphic top).

and show a better grouping of strike orientations (Fig. 4). The faults bounding tectonic lenses of different lithologies (Fig. 2) correspond to large-scale *Sh* faults which were the loci of important tectonic transport. The contacts between the tectonic units (Fig. 1) would represent the largest scale example of this fault set.

In the mudstones, the faults display shiny and finely striated surfaces. In the sandstones, the faults commonly show rough surfaces with weak striations; intensely striated shiny surfaces are rarer. In both lithologies, striated synkinematic calcite patches formed at releasing bends or steps of the fault surfaces are rare and usually do not exceed cm scale (A in Fig. 3b). Other classical second-order microstructures usable as shear-sense criteria (Petit & Laville 1987) are poorly developed on these faults. More common criteria are given by the offset of bedding or pre-existing faults (Figs. 2 and 3c & d). These kinematic indicators show that the directions and senses of movement are consistent for neighbouring *Sh* faults of a given outcrop (Fig. 4). In particular, the striation azimuth is relatively insensitive to changes of fault strike resulting from the curviplanar geometry of the faults. This resulted for numerous fault planes in a lateral component of movement; these planes having acted as 'lateral ramps' in the sigmoidal *Sh* fault network. The *Sh'* faults are dip-slip normal faults antithetic to the *Sh* faults, with an average striation azimuth similar to that of the latter (Fig. 4).

The faults of both sets cross-cut without forming sigmoidal geometry (Fig. 3b). Where offsets are present, they show that the *Sh'* faults are more commonly the later formed. Offsets along the *Sh'* faults are always much smaller than those along the corresponding *Sh* faults. On minor *Sh'* faults, offsets rarely exceed a few mm to cm. Thus, the *Sh'* faults are minor, commonly only incipient, and late structures with respect to the *Sh* faults.

The geometry and kinematics of the *Sh* and *Sh'* fault networks show that this deformation results from non-coaxial heterogeneous shear deformation. The *Sh* faults are synthetic to the general shearing and were the loci of tectonic transport. On a given outcrop, their average striation azimuth corresponds to the local shear direction and represents the local direction of tectonic transport. On the other hand, the antithetic *Sh'* faults do not correspond to a tectonic transport and only accommodated shear deformation. The angular relationship between the two sets of faults thus gives a shear-sense criterion. With reference to experiments on argillaceous sediments, the sigmoidal pattern of the *Sh* faults may have resulted from the anastomosing of *R*, *P* and *D* surfaces of the classic Riedel terminology (e.g. Tchalenko 1968, 1970). Our three-dimensional analysis shows that anastomosing of elementary surfaces occurs not only parallel to the shear direction but also transversely, along those planes having a lateral component of movement. The antithetic *Sh'* faults, which are well developed here, have only rarely been described in argillaceous sediments sheared experimentally (Arch *et al.* 1988, fig. 4a) or naturally (Koopman 1983, fig. 15, Labaume *et al.* 1990b). They are analogous to the *X* surfaces of the Riedel terminology.

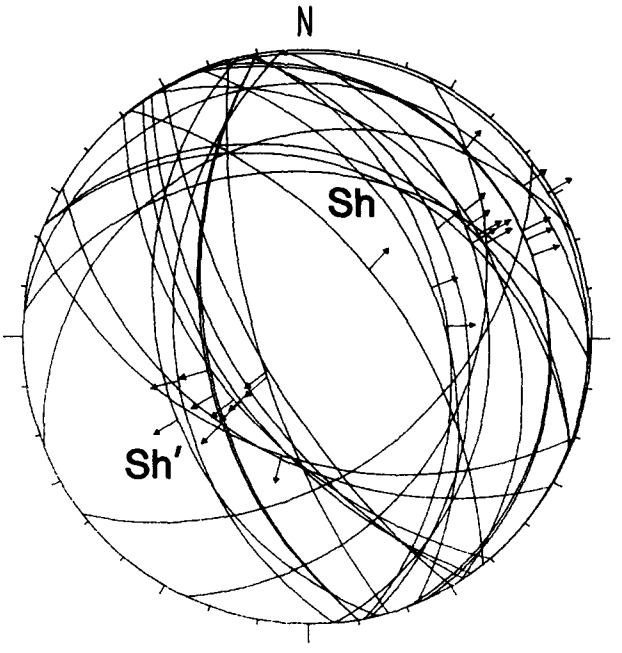

Fig. 4. Fault-slip data in *Sh*–*Sh'* fault network indicating low-angle shearing toward the northeast. The synthetic *Sh* faults dip gently toward the northeast and the antithetic *Sh'* faults dip steeply toward the southwest. Data collected on the outcrop shown in Fig. 3(a).

Scaly deformation bands

Locally, the concentration of shear deformation has resulted in the development of deformation bands which display a penetrative scaly fabric (Fig. 5). These scaly deformation bands are parallel to the *Sh* faults and their thickness ranges from a few cm up to more than 1 m. They have sharp boundaries formed by *Sh* faults. These are commonly offset by *Sh'* faults belonging to the *Sh–Sh'* fault network that occurs outside the deformation bands.

Inside a scaly deformation band, the fabric results from the interaction of two types of surfaces. The first set is a closely spaced *Sh* fault network where the geometry and sense of shearing are similar to those of the *Sh* faults situated outside the deformation band. In this network, the extensional *R* Riedel surfaces are common. The second set of surfaces consists in a penetrative foliation (*S*-microfabric) inside the lenses of rock isolated by the *Sh* network. The *S*-microfabric dips in the sense opposite to the *Sh* fault vergence, with an angle varying from about 20° to 50° with respect to the average deformation band orientation. The *S*-microfabric shows a sigmoidal geometry compatible with the *Sh* fault vergence, thus giving a very efficient shear-sense criterion. The *S*-surfaces are usually shiny and display fine striation parallel to that on the *Sh* faults. In thin section, the *S*-microfabric is marked by a preferred alignment of platy grains (B in Fig. 6c). It differs from the *Sh'* faults located outside the deformation band by its penetrative character and sigmoidal geometry.

Similar microfabrics have already been described, with diverse terminologies, for shear zones in argillaceous sediments deformed naturally (e.g. Koopman 1983, Cowan *et al.* 1984, Rutter *et al.* 1986, Chester & Logan 1987, Behrmann *et al.* 1988, Platt *et al.* 1988, Agar *et al.* 1989) and experimentally (Tchalenko 1968, Rutter *et al.* 1986). Because of geometrical similarities, the *Sh–S* pattern is often compared to the *C–S* pattern of mylonitic shear zones in metamorphic rocks (Berthé *et al.* 1979, Lister & Snoke 1984). However, although the works cited above show that the *S*-microfabric in argillaceous sediments results from grain reorientation, its exact significance in the strain field and the kinematics of its development remain unresolved. Two alternative origins have been proposed, i.e. the microfabric may represent a flattening fabric, possibly reactivated as slip surfaces by late flow partitioning, or it may originate as closely spaced microshear zones (see Behrmann *et al.* 1988 for review).

Relationships with the regional nappe structure

At the regional scale, kinematic analysis of the *Sh–Sh'* fault networks and scaly deformation bands indicates a low-angle shearing toward the northeast which corresponds to the shear deformation associated with nappe emplacement (Labaume *et al.* 1990a).

The lithology and structural position did not influence notably the basic geometry of the shear structures. However, these factors may explain why the distribution and the intensity of the deformation are very heterogeneous (Fig. 3). In the turbidites of the Bobbio Formation, the shear deformation is restricted in the few metres to tens of metres below the sole thrust of the Coli Unit. The shear structures cut the normal and reverse limbs of the large syncline (section in Fig. 1) with similar orientations, showing they are post-folding features which formed when the Coli Unit sole thrust cut the syncline (Figs. 3c & d). The Coli Unit is made of mudstones more deformable than the turbidites of the Bobbio Formation and is squeezed between under- and overlying units. This explains why the shear deformation occurs within the whole unit. However, the deformation is particularly intense (and with more abundant and thicker scaly deformation bands) near the major tectonic contacts defined by mapping (Labaume *et al.* 1990a).

CALCITE VEINS IN SHEAR STRUCTURES

Calcite vein arrays are commonly associated with the *Sh–Sh'* fault networks and the scaly deformation bands. The most common veins are tabular bodies which reach 1–5 cm in thickness and several metres to tens of metres in length (Figs. 6a & b). These veins are referred to as 'tabular calcite veins'. They display various strikes and dips but, except in locally complex areas, most of them have low dips and are sub-parallel with the local *Sh* faults or intercalated within the scaly deformation bands (Fig. 6a & b).

Geometry and mechanism of vein opening

The tabular calcite veins are bounded by striated shear surfaces (Fig. 7). Individual tabular calcite veins are usually formed of several superposed 'elementary' calcite sheets a few mm to cm thick bounded by striated surfaces. Striation on individual surfaces are usually rectilinear, but it is common that the different surfaces within an individual tabular calcite vein display different striation directions. The shear surfaces bounding individual calcite sheets form parallel planes on sections parallel to the striation, but they are usually curviplanar and form an anastomosed network on sections perpendicular to the striation.

Internal microstructures show that each 'elementary' calcite sheet is a shear vein, i.e. it results from calcite crystallization in a great number of rhomb-shaped cavities which correspond to releasing oversteps between the two bounding shear surfaces (Fig. 7). The acute angle between the shear surfaces and the initial rupture responsible for each overstep indicates unambiguously the shear sense. This angle suggests a mode I rupture, i.e. rupture occurred sub-parallel to the local direction of the maximum principal stress σ_1. The direction of the subsequent opening was controlled by the movement along the shear surfaces.

Many tabular calcite veins show the superposition of two types of releasing oversteps which both indicate the

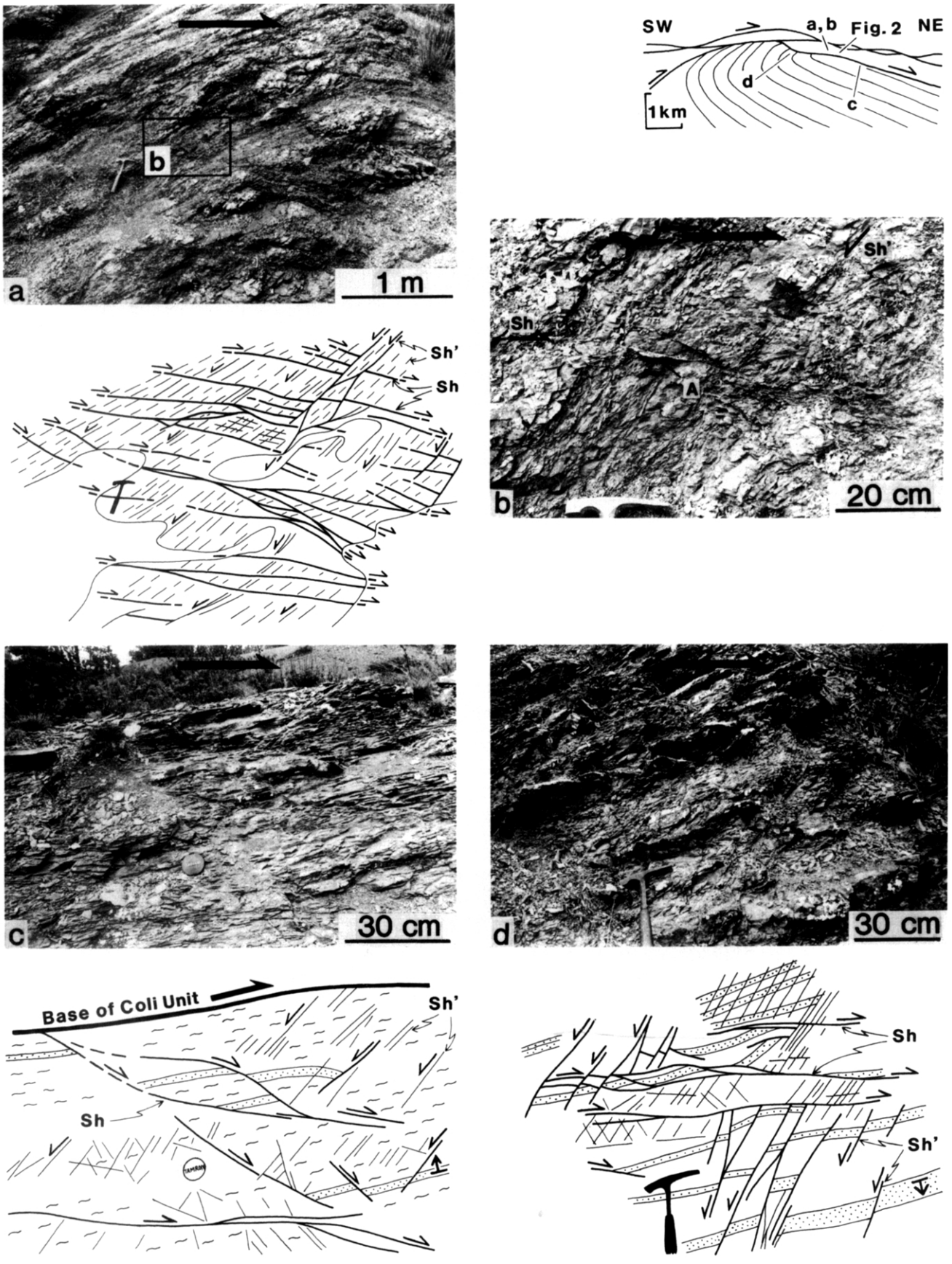

Fig. 3. *Sh–Sh'* fault networks in various lithologies and structural positions (inset at top right: structural position of the outcrops in section of Fig. 1). *Sh* and *Sh'*, respectively, synthetic and antithetic faults with respect to the general shearing towards the northeast (to the right on all photographs). (a) Intense shearing in mudstones of the Coli Unit (on this outcrop, bedding is obliterated by the closely-spaced fracturing; box: photograph b). (b) Detail of (a) (A: striated calcite patch). (c) Shearing in right-way-up fine-grained turbidites of the Bobbio Formation, at the contact of the Coli Unit sole thrust (in this example, footwall deformation is weak and restricted to a few metres below the major contact, and the *Sh* faults assume the position of *R* Riedel surfaces with respect to the latter). (d) Shearing in inverted fine-grained turbidites of the Bobbio Formation, 20 m below the Coli Unit sole thrust.

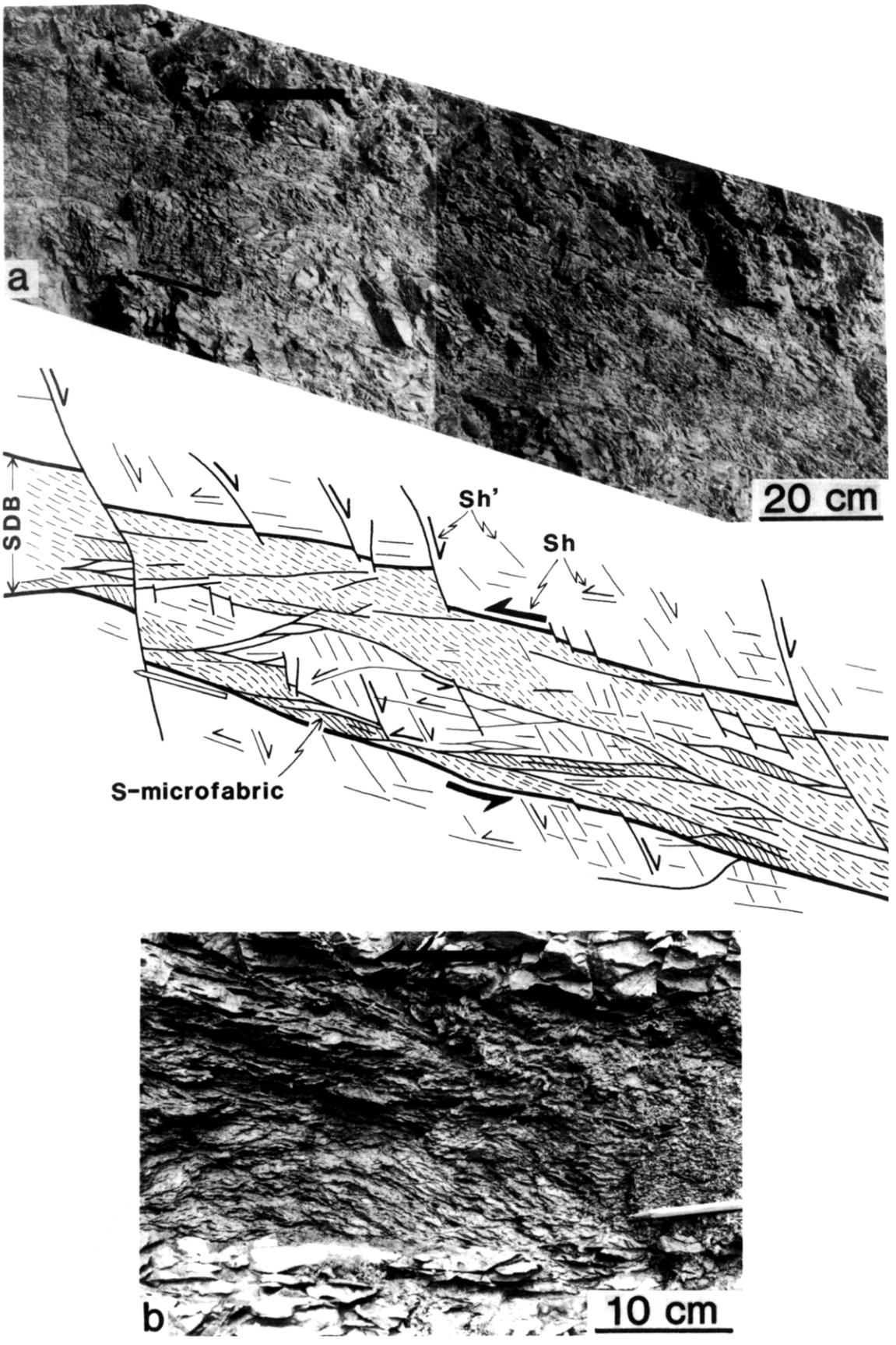

Fig. 5. Scaly deformation bands (SDB) in mudstones of the Coli Unit. *Sh* and *Sh'*, respectively, synthetic and antithetic faults with respect to the general shearing towards the northeast (to the left on both photographs). (a) General view. (b) Detailed view.

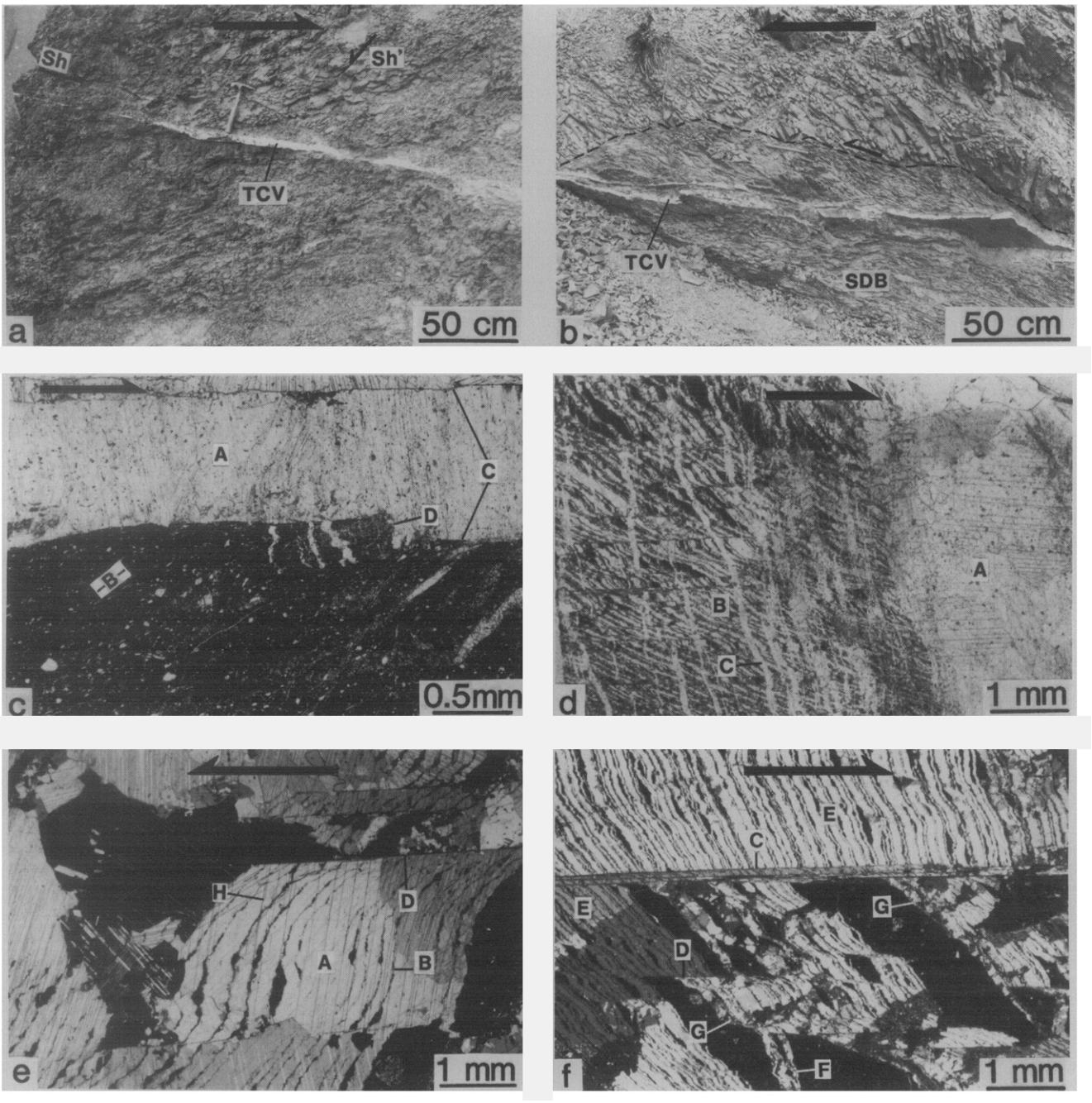

Fig. 6. (a) & (b) Tabular calcite veins (TCV) in sheared mudstones of the Coli Unit, intercalated in a *Sh–Sh'* fault network (a) or in a scaly deformation band (SDB) (b). In both cases, the TCV microstructures indicate the same sense of shearing as the previously formed shear structures (towards the northeast, to the right in a and to the left in b). (c) & (d) Chronologies of TCV microstructures. (c) Part of a releasing overstep (A) opened across previously formed *S*-microfabric (B) in sediment of a SDB: (C) shear surfaces bounding the releasing overstep (note slight late stylolitization of the upper shear surface): (D) step cutting the *S*-microfabric; geometry of the *S*-microfabric and of the overstep both indicate shearing toward the right. (d) Part of a large secondary releasing overstep (A) cutting previously formed crack–seal vein sequences (B): (C) minor veins associated with the secondary opening; the wall of the secondary opening dips more steeply than the crack–seal vein walls, and both dips indicate shearing toward the right. (e) & (f) Geometry and calcite-fill fabrics of crack–seal vein sequences. (A) Calcite-fill of the crack–seal veins; (B) matrix bands; (C) shear surfaces; (D) transform faults (cf. Figs. 9a–c); shearing is towards the left in (e) and towards the right in (f). In (e), large calcite crystals display an irregular fabric and segmented contacts indicating face-controlled growth of crystals; note twinning of the crystals (H). In the lower part of (f), face-controlled growth of the crystals resulted in an incipient fibrous fabric perpendicular to the matrix bands (i.e. oblique to the shear movement, which is parallel with the shear surfaces and transform faults). Large crystals (E) occur in areas displaying thin matrix bands and small crystals (F) occur between thick matrix bands; small crystals at the right-hand side of the thick matrix bands (G) pass laterally to larger crystals, indicating that younger veins are toward the right (see discussions in the text).

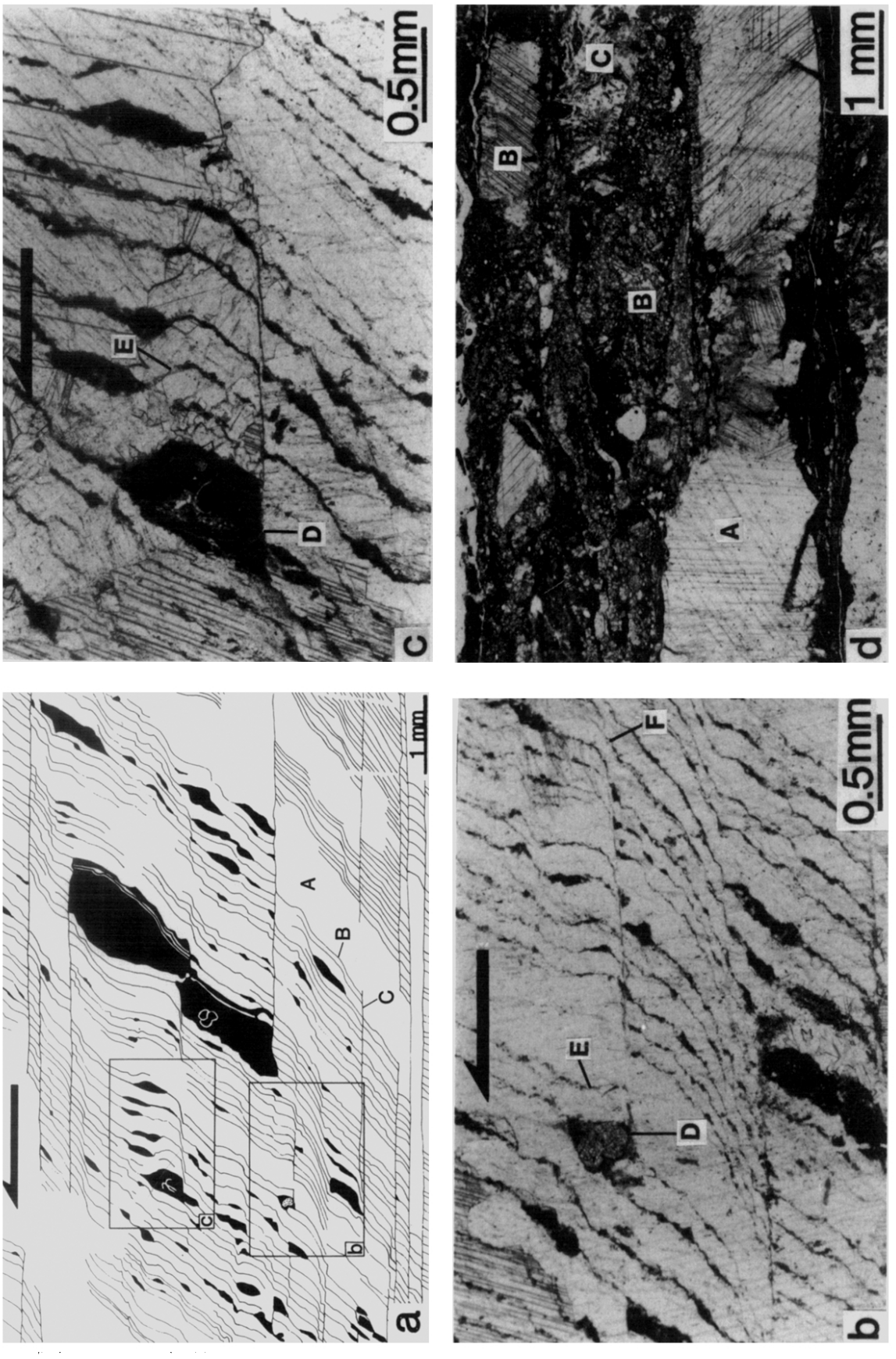

Fig. 9. (a)–(c) Transform faults in crack–seal vein sequences of tabular calcite vein. Shearing is toward the left. (A) calcite fill of the crack–seal veins; (B) matrix bands; (C) transform faults. Fossil debris form heterogeneities responsible for initiation of transform faults (D) and the dip of matrix bands locally opposite to the general dip (E); these abnormal dips are attenuated toward the right, as well as the transform faults (F). These features indicate that the veins are younger towards the right. The transform fault is parallel with the shear movement in (b) and slightly oblique in (c). (d) Boudinage of a tabular calcite vein. At bottom, a calcite tablet (A) is boudinaged by combination of pressure solution and intense twinning. Above, completion of boudinage resulted in melange of disaggregated calcite crystals and sediment matrix (B); (C) post-boudinage calcite crystallization. Note that sediment was still deformable enough to flow during boudinage.

same sense of shearing (Figs. 6d and 7). They are distinguished by their relative chronology and their overall geometry.

The first generation of releasing oversteps consists of sequences of a great number of narrow calcite veins separated by thin bands of encasing sediment ('matrix bands') and bounded by closely spaced (<5 mm) shear surface ('crack–seal vein sequences' in Figs. 6d–f and 7). On the shear surfaces, the matrix bands form parallel sinuous septae (Platt *et al.* 1988, fig. 13b). Each vein corresponds to a small releasing overstep which width varies from 0.025 to 1 mm, most common values being around 0.05 mm. For each vein, the shape-ratio between the length of initial rupture and the opening width (Fig. 8) is thus usually largely in excess of 10. Matrix bands are usually extremely thin with respect to the adjacent veins and are locally discontinuous. The angle between the shear surfaces and the vein sequences varies between extreme values of 20° and 80°, most common values ranging between 50° and 60°. The regularly repetitive geometry of the vein sequences indicates a 'crack–seal' mechanism of deformation (Ramsay 1980, Ramsay & Huber 1983, Gaviglio 1986) (Fig. 8). The veins were formed sequentially, the opening of each releasing overstep occurring only after the crystallization of calcite in the previously formed neighbouring overstep. The presence of the matrix bands shows that the successive ruptures occurred preferentially in the sediment rather than exactly at the calcite–sediment interface. This may be due to an incomplete cementation of the very fine-grained sediment (see Discussion below), allowing the sediment porosity to be invaded by the calcite vein fill close to the vein walls. During the following rupture, this thin band of sediment 'impregnated' by the calcite remained 'stuck' to the latter, thus forming the matrix band separating the neighbouring veins. The crack–seal vein sequences are commonly offset by a few tenths of mm by transform faults sub-parallel with the shear surfaces (Figs. 9a–c). In some cases, one can observe that these transform faults were initiated by heterogeneities (e.g. a fossil debris or a 'large' siliciclastic grain) which locally hardened the sediment, thus deviating the rupture trajectory (D in Figs. 9b & c). These peculiar structures indicate the younging direction of the vein sequence formation. The veins can branch on the shear surfaces or transform faults with variable geometries (Figs. 9a–c) which cannot be related to a simple model of stress deviation at the tip of shear surface (Gaviglio 1986). In some cases, these geometries are obviously dependent on heterogeneities in the sediment (Figs. 9a–c).

The second generation of releasing oversteps corresponds to larger (commonly several cm across) calcite-filled domains that do not form repetitive sequences and cross-cut the previously formed crack–seal vein sequences (Figs. 6c–d and 7). The spacing between the bounding shear surfaces is usually in the order of 1–3 cm, and shear displacement can be more than several cm or dm. This corresponds to an initial rupture length/opening width shape-ratio much smaller than 1. The initial ruptures of these secondary oversteps are longer and form a larger angle with the shear surfaces than those of the crack–seal veins (Fig. 6d and A in Fig. 7). Where similar secondary releasing oversteps opened in the sediment (B in Fig. 7), the initial ruptures may have corresponded to irregular crack networks. It results in vein networks which separate sediment elements forming breccia-like accumulations close to the releasing

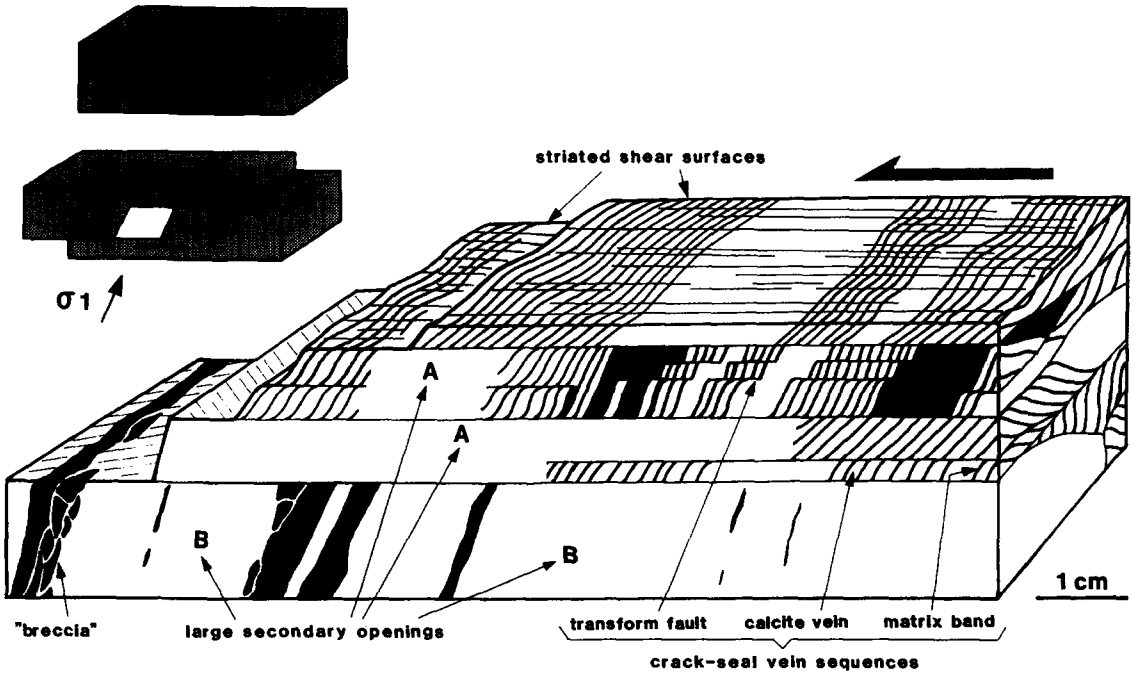

Fig. 7. Anatomy of a tabular calcite vein resulting from multiple releasing overstep openings between shear surfaces (shearing is towards the left). The sediment is in black (internal fabric is not shown) and the calcite-fill is in white (crystal boundaries are not shown). (A) Large secondary oversteps opened across previously formed crack–seal vein sequences; (B) as (A) but opened in the sediment. Scale is approximate and crack–seal vein width is exaggerated. Top left: principle of releasing overstep opening (see also Fig. 8); sediment is in grey and calcite is in white.

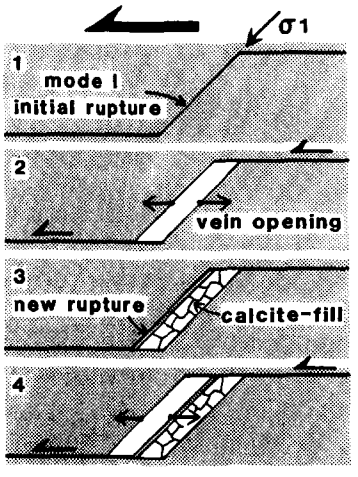

Fig. 8. Sequence of crack–seal vein formation. Each vein corresponds to a releasing overstep opened during an increment of shear movement, and was sealed by calcite crystallization before the following increment which opened the neighbouring vein.

overstep walls (Fig. 7). In some cases, inclusion bands of this type isolated in the calcite-fill (Fig. 7) suggest an incremental opening mechanism.

Calcite crystallization in the tabular calcite veins

In the releasing oversteps of both generations, a striking feature is the usual lack of fibrous fabric parallel to the shear displacement in the calcite-fill (Figs. 6e & f), contrary to usual examples of shear veins (e.g. Ramsay & Huber 1983, Gaviglio 1986 and many others).

In the crack–seal vein sequences, fabric of the calcite crystals is usually irregular. Optical measurements show that this fabric corresponds to a random orientation of the optical axes of the crystals. Those areas where the matrix bands are very thin, locally discontinuous, usually show 'large' crystals (up to several mm across) which include numerous crack–seal increments (Figs. 6e & f). This shows that these thin bands were not an obstacle to optical continuity of calcite crystallization. This allowed a few crystals to be developed preferentially during a great number of successive increments, thus inhibiting the growth of the new small crystals which can be observed against the matrix bands. The boundaries between adjacent crystals commonly show a segmented geometry indicating control of their growth by the various surfaces of the vein pattern (Figs. 6e & f). Crystal faces are usually parallel either to the shear surfaces, or to the vein walls, or they are perpendicular to one of these two directions. An incipient fibrous fabric may be developed in zones where one of these directions is locally prevalent (Fig. 6f). 'Small' crystal (a few tens of microns) calcite-fills are rather rare and usually occur associated with thick matrix bands (Fig. 6f). This indicates that these thick bands isolated enough veins to allow their calcite-fill to develop out of the influence of crystals already dominant in the previously formed neighbouring veins. Where a thick matrix band occurs isolated within a sequence of thin bands, the thick band is commonly bounded on one side by numerous small crystals which pass laterally to progressively less numerous and larger crystals (G in Fig. 6f). This results from the crystal competition allowed by the thin bands and indicates the younging direction of the vein formation. In an individual crack–seal vein sequence, this criterion always indicates the same younging direction, and it is compatible with that given by the transform faults (cf. right-hand side of the fossil debris, D in Fig. 9c). These features confirm that the fabric of the calcite-fill is an original one and does not result from post-tectonic recrystallization.

In the large secondary releasing oversteps, the calcite-fill is usually made of large crystals displaying an irregular fabric. We have found only two cases where a classic fibrous fabric tracks the path of opening. In the case where a secondary releasing overstep is superposed on an earlier crack–seal vein sequence, its calcite-fill is in optical continuity with that of the crack–seal veins.

In thin section, the calcite crystals show a well defined extinction between crossed polarizers. They are usually intensely twinned on the *e* planes $\{01\bar{1}2\}$ (Fig. 6e). The twin lamellae are straight and sharply defined, and their width is less than a micron, which corresponds to a slight deformation of the crystals ($\simeq$1%). Dynamic analysis of the twin lamellae by the method of Laurent *et al.* (1990) has been carried out on some veins and will be reported in a separate paper. The most striking result is that, for each sample, the stress orientation compatible with most of the twins is also compatible with the shear sense deduced from the vein geometry, showing that twinning began relatively early. For low *P–T* conditions, there are no optical means to distinguish deformation twins from growth twins (Laurent *et al.* 1990). In the present case, the interpretation of most of the twins as deformation twins is supported by the results of the dynamic analysis.

Late deformation of the tabular calcite veins

During continuation of the shear deformation, the tabular calcite veins may have undergone late deformations which consist mainly of boudinage (Fig. 9d) or folding. In these structures, localized deformation of the calcite crystals involves a combination of pressure solution (stylolites), intense twinning on the *e* planes $\{01\bar{1}2\}$ and gliding on the *r* planes $\{10\bar{1}1\}$. In the case of boudinage, the interboudin domains may have been filled either by new calcite crystals, or by flowing of the encasing sediment (Fig. 9d), depending on the ability of the latter to undergo particulate flow. Completion of this process may have led to locally disaggregated calcite sheets, now forming a disorganized melange of sediment and 'floating' calcite crystals (Fig. 9d). These late deformations were probably controlled by the rheological contrast between the competent calcite sheets and the more deformable encasing sediment. In many tabular calcite veins, another type of late deformation consists of the stylolitization of the shear surfaces after the shear movement has ceased (Fig. 6c).

Relationships with the regional nappe structure

Microstructural relationships show that the formation of the tabular calcite veins is after that of the *Sh–Sh'* fault networks and scaly deformation bands (Fig. 6c).

The tabular calcite vein microstructures indicate a general movement toward the northeast, compatible with that deduced from the *Sh–Sh'* fault networks and scaly deformation bands. However, at the outcrop scale, the striation azimuth of the tabular calcite veins commonly departs more or less from that of the *Sh–Sh'* fault networks and scaly deformation bands. This is consistent with the fact that the two types of structures were not formed simultaneously. Dispersion of striation azimuth between the diverse calcite sheets of individual tabular calcite veins also marks a difference from the greater regularity of shear direction indicated by the *Sh–Sh'* faults and scaly deformation bands. This dispersion does not seem to record global changes in direction of nappe emplacement, but would rather correspond to local erratic perturbations within the general nappe movement. These may have resulted from deviations of movement imposed on the low-dipping faults by neighbouring steep-dipping transverse faults.

DISCUSSION

At any scale, the structures and microstructures described correspond to heterogeneous strains and displacements. In the absence of strain markers, the most striking feature is the evolution of the deformation structures in time (Fig. 10). This indicates changes of deformation mechanisms which are most probably related to modifications of the mechanical properties of the sediment in response to its progressive compaction and dewatering. This would be compatible with the regional context which shows that the sediments were involved in active tectonics as soon as they were deposited, implying that deformation was at least partly syn-diagenetic.

The first-formed structures are the *Sh–Sh'* fault networks and scaly deformation bands which correspond to heterogeneous ductile flow achieved by particulate flow. This mechanism is characteristic of deformation of weakly lithified sediment (Knipe 1986). It is attested here by the *S*-microfabric in the scaly deformation bands and by the typical morphologies of the fault surfaces, quite analogous to those described in many examples of soft-sediments deformed experiment-

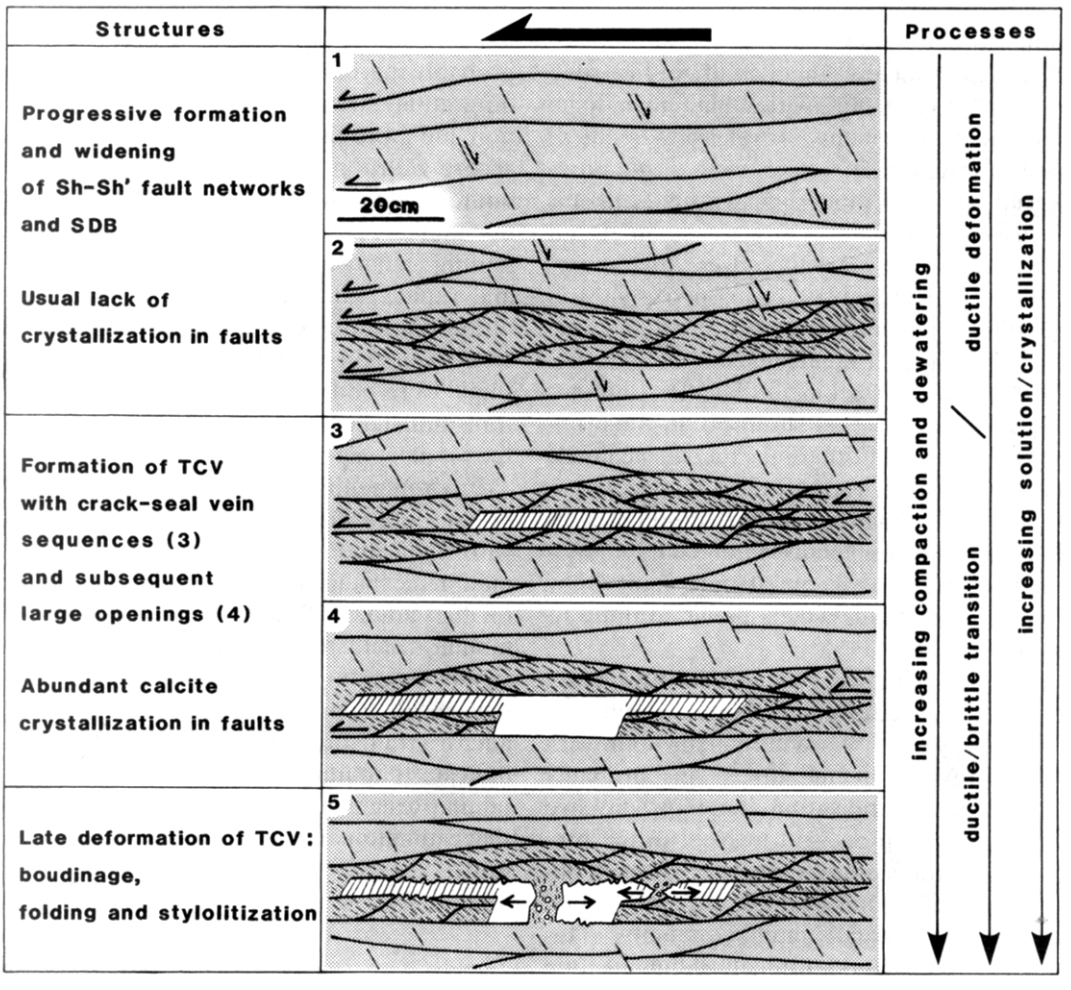

Fig. 10. Summary of evolution of structures and deformation mechanisms during progressive shear deformation. *Sh* and *Sh'*, respectively, synthetic and antithetic faults with respect to the general shearing; SDB, scaly deformation bands; TCV, tabular calcite veins. In the middle column, shearing is toward the left, sediment is in grey and calcite of TCV is in white.

ally (e.g. Maltman 1987, Will & Wilson 1989) or naturally in various geodynamic contexts (e.g. Guiraud & Séguret 1987, Petit & Laville 1987, Labaume *et al.* 1990b). Low finite displacements on most of the individual faults forming the closely-spaced *Sh–Sh'* fault network show that each fault was locked early after its formation. This may be possibly due to a strain-hardening process operating in the vicinity of the newly formed faults. This process, already proposed for formation of scaly fabrics and stratal disruption (Karig 1986, Moore *et al.* 1986, Moore & Byrne 1987), may result from grain collapse and associated expulsion of interstitial water during faulting, and would be responsible for progressive widening of deformed zones. This stage of deformation would thus also correspond to an episode of compaction and dewatering of the sediment. Water drainage was probably achieved preferentially along the fault network, where fracture permeability was higher than the sediment permeability (Moore *et al.* 1988, Moore 1989). In this network, the anastomosed *Sh* faults and scaly deformation bands probably formed the main, gently dipping path for long-distance water expulsion. During this stage of deformation, calcite crystallization usually did not occur along the fault surfaces. This suggests that in weakly lithified and water-saturated sediment, the thermodynamical conditions for solution and/or crystallization were not reached. Lack of crystallization may be also related to the inability of the weak sediment to maintain open the cavities that tended to be formed during fault movements, at releasing bends of fault surfaces for instance. By reference to *in situ* pore-pressure measurements in modern accretionary prisms (Moore *et al.* 1982, Von Huene 1985), we can infer that deformation was probably facilitated by high pore-pressure (Hubbert & Rubey 1959) developed as a result of tectonic loading applied to water-saturated and low-permeability soft sediment (Von Huene & Lee 1982, Shi & Wang 1988) during the stacking of the allochthonous units. In these conditions of weak lithification and probable high pore-pressure, deformation could be achieved under very low differential stresses and effective principal stresses, and displacements along the low-dipping *Sh* faults and scaly deformation bands were facilitated by a very low level of friction. These ductile faults may correspond to aseismic faults which moved at more or less constant strain rate.

The tabular calcite veins were formed after the *Sh–Sh'* fault networks and scaly deformation bands. Their main feature is the occurrence of fracture behaviour with respect to the previous ductile flow. This probably resulted from increased lithification, due to progressive compaction and cementation, with respect to the previously formed structures. Another feature of the tabular calcite veins is the concentration of large finite displacements on a restricted number of faults. This indicates that, in sufficiently lithified sediment, the difference in the strength of the existing fault-zones compared to the unfaulted sediment facilitated these large displacements rather than the creation of new faults. Abundant calcite crystallization gives direct evidence of important water flow along the gently dipping fault networks and attests that the conditions for solution/crystallization were reached. Veins also indicate that cavities may be maintained open, due to sufficient rigidity of the sediment or/and high enough pore-pressure. A SW-dipping solution cleavage, compatible with the general shearing linked with nappe emplacement, is locally present in the Oligo-Miocene sediments of the Bobbio window. Its spatial distribution is very irregular and cannot be correlated with that of the other shear structures. Nevertheless, the calcite crystallized in the tabular calcite veins may be related in part to the formation of this solution cleavage. The opening of large releasing oversteps across previously formed crack–seal vein domains was also dependent on mechanical behaviour of the ruptured material. Indeed, these openings occurred across aggregates of calcite crystals, differing from the crack–seal veins which were formed in the sediment. This resulted in a larger acute angle between the initial rupture and the shear surfaces for these late openings than for the previous crack–seal veins, due to greater rigidity of the ruptured material (A in Fig. 7). By analogy, we can suggest that the opening of large releasing oversteps in the sediment was also dependent on hardening of this sediment with respect to the previous stage of crack–seal vein formation (B in Fig. 7). The progressive consolidation of the sediment probably permitted the build up of relatively large differential stresses during tabular calcite vein formation, and pore-pressure may have been lower. This is in accord with the fact that the releasing oversteps could not form without some level of friction. We suggest that the tabular calcite veins may correspond to 'seismic faulting', characterized by discontinuous displacements and rapid strain rate events, associated to drops of differential stresses and stored elastic energy. The crack–seal vein sequences probably correspond to very small drops of differential stress and may correspond to transitional ductile–brittle behaviour at the beginning of the tabular calcite vein formation.

Environmental tectonic parameters such as the pore pressure and the strain rate may have also interacted with lithification in controlling the evolution of deformation mechanisms. This may be particularly important for the sediment flow associated with boudinage of the tabular calcite veins. Indeed, this behaviour corresponds to a return in the field of particulate flow which may result from a transient increase in pore pressure and/or strain rate (Knipe 1986, Labaume 1987). This indicates that lithification was still only partial when the tabular calcite veins were formed, and emphasizes that estimation of deformation parameters is only qualitative.

CONCLUSIONS

Shear structures of the 'Bobbio window' illustrate the style of shear deformation possible in accretionary prisms.

The early formed *Sh–Sh'* fault networks and scaly deformation bands attest to deformation of poorly compacted and dewatered sediments, and evolution of these structures was probably dependent on progressive compaction and dewatering of the sediment. Later formation of the tabular calcite veins is thought to indicate important lithification in the latest stages of deformation. Evolution of the deformation style would thus accompany the progressive consolidation of the sediment inferred in modern accretionary prisms from seismic velocities (Bray & Karig 1985, Fowler *et al.* 1985) and from porosity measurement on drill-core samples (e.g. Moore 1989). Insufficient lithification may be responsible for the lack of thick and extensive mineralized veins in the sheared sediments at the toe of modern accretionary prisms. This is for example the case for the still soft sheared Quaternary marly clays of the Catania foredeep (Sicily), which display *Sh–Sh'* fault networks quite analogous to those described here, but lack any mineralized veins (Labaume *et al.* 1990b).

The geometry of the structures described illustrates also the drainage network of interstitial water in accretionary prisms. In particular, it is shown that the gently-dipping faults form a major interconnected drainage pattern analogous to that formed by the shear zones in modern prisms.

The geometrical and kinematic analysis of the structures from the mm to the tens of metres scale has also defined shear criteria useful for analysis of prism emplacement. In particular, recognition of the *Sh–Sh'* fault networks allows analysis of *a priori* complex fracture networks. Similarly, recognition of vein arrays opened by crack–seal mechanism gives the most frequent (in most cases the only one) and most reliable shear criterion for determining the kinematics of the tabular calcite veins.

Acknowledgements—We thank M. Séguret who stimulated our interest for the calcite veins in superficial nappe tectonics and criticized early drafts of the manuscript. We also thank R. Knipe and another anonymous referee for their constructive reviews, and D. Mainprice for correction of the English text. Field work was supported by a geological mapping contract with the "Regione Emilia-Romagna" (Bologna, Italy).

REFERENCES

Abbate, E., Bortolotti, V., Maxwell, J. C., Merla, P., Passerini, P., Sagri, M. & Sestini, G. 1970. Development of the Northern Apennines geosyncline. *Sediment. Geol.* **4**, 201–648.

Agar, S. M., Prior, D. J. & Behrmann, J. H. 1989. Back-scattered electron imagery of the tectonic fabrics of some fine-grained sediments: implications for the fabric nomenclature and deformation processes. *Geology* **17**, 901–904.

Arch, J., Maltman, A. J. & Knipe, R. J. 1988. Shear-zone geometries in experimentally deformed clays: the influence of water content, strain rate and primary fabric. *J. Struct. Geol.* **10**, 91–99.

Behrmann, J. H., Brown, K., Moore, J. C., Mascle, A., Taylor, E., Alvarez, F., Andreieff, P., Barnes, R., Beck, C., Blanc, G., Clark, M., Dolan, J., Fisher, A., Gieskes, J., Hounslow, M., McLellan, P., Moran, K., Ogawa, Y., Sakai, T., Schoonmaker, J., Vrolijk, P., Wilkens, R. & Williams, C. 1988. Evolution of structures and fabrics in the Barbados Accretionary Prism. Insights from Leg 110 of the Ocean Drilling Program. *J. Struct. Geol.* **10**, 577–591.

Bellinzona, G., Boni, A., Braga, G., Casnedi, R. & Marchetti, G. 1968. Carta geologica della "Finestra" di Bobbio. *Atti Ist. Geol. Univ. Pavia* **XIX**.

Berthé, D., Choukroune, P. & Jegouzo, P. 1979. Orthogneiss mylonite and non coaxial deformation of granites: the example of the South-Armorican shear zone. *J. Struct. Geol.* **1**, 31–42.

Boccaletti, M., Elter, P. & Guazzone, G. 1971. Plate tectonics model for the development of the Western Alps and the Northern Apennines. *Nature, Phys. Sci.* **234**, 108–111.

Bray, J. C. & Karig, D. E. 1985. Porosity of sediments in accretionary prisms and some implications for dewatering processes. *J. geophys. Res.* **90**, 768–778.

Chester, F. M. & Logan, J. M. 1987. Composite planar fabric of gouge from the Punchbowl Fault, California. *J. Struct. Geol.* **9**, 621–634.

Cloos, M. 1984. Landward-dipping reflectors in accretionary wedges: active dewatering conduits? *Geology* **12**, 519–522.

Cowan, D. S., Moore, J. C., Roeske, S. M., Lundberg, N. & Lucas, S. E. 1984. Structural features at the deformation front of the Barbados Ridge Complex, Deep Sea Drilling Project Leg 78A. *Init. Reps DSDP, Washington* (U.S. Govt Printing Office), **LXXVIII**, 535–548.

Elter, P. 1973. Lineamenti tettonici ed evolutivi dell'Appennino. In: *Moderne vedute sulla geologia dell'Appennino. Acad. Naz. Lincei. Roma* **183**, 97–109.

Fisher, D. & Byrne, T. 1987. Structural evolution of underthrust sediments, Kodiak Islands, Alaska. *Tectonics* **6**, 775–793.

Fowler, S. R., White, R. S. & Louden, K. E. 1985. Sediment dewatering in the Makran accretionary prism. *Earth Planet. Sci. Lett.* **75**, 427–438.

Gaviglio, P. 1986. Crack–seal mechanism in a limestone: a factor of deformation in strike-slip faulting. *Tectonophysics* **131**, 247–255.

Guiraud, M. & Séguret, M. 1987. Soft-sediment microfaulting related to compaction within the fluvio-deltaic infill of the Soria strike-slip basin (northern Spain). In: *Deformation of Sediments and Sedimentary Rocks* (edited by Jones, M. E. & Preston, R. M. F.). *Spec. Publs geol. Soc. Lond.* **29**, 123–136.

Henry, P., Lallemant, S. J., Le Pichon, X. & Lallemand, S. E. 1989. Fluid venting along Japanese trenches: tectonic context and thermal modelling. *Tectonophysics* **160**, 277–291.

Hubbert, M. K. & Rubey, W. W. 1959. Role of fluid pressure in the mechanics of overthrust faulting. I: Mechanics of fluid-filled porous solids and its application to overthrust faulting. *Bull. geol. Soc. Am.* **70**, 115–166.

Karig, D. E. 1986. Physical properties and mechanical state of accreted sediments in the Nankai Trough, Southwest Japan Arc. In: *Structural Fabrics in Deep Sea Drilling Project Cores from Forearcs* (edited by Moore, J. C.). *Mem. geol. Soc. Am.* **166**, 117–133.

Kligfield, R. 1979. The Northern Apennines as a collisional orogen. *Am. J. Sci.* **279**, 676–691.

Knipe, R. J. 1986. Deformation mechanism path diagrams for sediments undergoing lithification. *Mem. geol. Soc. Am.* **166**, 151–160.

Koopman, A. 1983. Detachment tectonics in the Central Apennines, Italy. *Geol. Ultraiectina* **30**, 1–155.

Labaume, P. 1987. Syn-diagenetic deformation of a turbiditic succession related to submarine gravity nappe emplacement, Autapie Nappe, French Alps. In: *Deformation of Sediments and Sedimentary Rocks* (edited by Jones, M. E. & Preston, R. M. F.). *Spec. Publs geol. Soc. Lond.* **29**, 147–164.

Labaume, P., Mutti, E., Rio, D. & Fornaciari, E. 1990a. Geometria e struttura de la Formazione di Bobbio (Appennino emiliano): relazione a la messa in posto dell'Unità di Canetolo. Seminario "Progetto Cartografia Geologica", Regione Emilia-Romagna, 21–23 Feb., Bologna (abs.).

Labaume, P., Bousquet, J. C. & Lanzafame, G. 1990b. Early deformation at a submarine compressive front: the Quaternary Catania foredeep south of Mt. Etna, Sicily, Italy. *Tectonophysics* **177**, 349–366.

Lash, G. G. 1989. Documentation and significance of progressive microfabric changes in Middle Ordovician trench mudstone. *Bull. geol. Soc. Am.* **101**, 1268–1279.

Laurent, Ph, Tourneret, C. & Laborde, O. 1990. Determining deviatoric stress tensors from twin lamellae in calcite. Applications to monophased synthetic and natural polycrystals. *Tectonics* **9**, 379–389.

Lister, G. S. & Snoke, A. W. 1984. S–C mylonites. *J. Struct. Geol.* **6**, 617–638.

Maltman, A. J. 1987. Shear-zones in argillaceous sediments: an experimental study. In: *Deformation of Sediments and Sedimentary Rocks* (edited by Jones, M. E. & Preston, R. M. F.). *Spec. Publs geol. Soc. Lond.* **29**, 77–87.

Moore, J. C. 1989. Tectonics and hydrogeology of accretionary prisms: role of the décollement zone. *J. Struct. Geol.* **11**, 95–106.

Moore, J. C., Biju-Duval, B., Bergen, J. A., Blackington, G., Claypool, G. E., Cowan, D. S., Duennebier, F., Guerra, R. T., Hemleben, C. H. J., Hussong, D., Marlow, M. S., Natland, J. H., Pudsey, C. J., Renz, G. W., Tardy, M., Willis, M. E., Wilson, D. & Wright, A. A. 1982. Offscraping and underthrusting of sediment at the deformation front of the Barbados Ridge: Deep Sea Drilling Project Leg 78A. *Bull. geol. Soc. Am.* **93**, 1065–1077.

Moore, J. C. & Byrne, T. 1987. Thickening of fault zones: a mechanism of melange formation in accreting sediments. *Geology* **15**, 1040–1043.

Moore, J. C., Mascle, A., Taylor, E., Andreieff, F., Alvarez, F., Barnes, R., Beck, C., Behrmann, J., Blanc, G., Brown, K., Clark, M., Dolan, J., Fisher, A., Gieskes, J., Hounslow, M., McLellan, P., Moran, K., Ogawa, Y., Sakai, T., Schoonmaker, J., Vrolijk, P., Wilkens, R. & Williams, C. 1988. Tectonics and hydrogeology of the northern Barbados Ridge: results from Ocean Drilling Program Leg 110. *Bull. geol. Soc. Am.* **100**, 1578–1593.

Moore, J. C., Roeske, S., Lundberg, N., Schoonmaker, N., Cowan, D. S., Gonzales, E. & Lucas, S. E. 1986. Scaly fabrics from Deep Sea Drilling Project cores from forearcs. In: *Structural Fabrics in Deep Sea Drilling Project Cores from Forearcs* (edited by Moore, J. C.). *Mem. geol. Soc. Am.* **166**, 55–73.

Mutti, E. & Ghibaudo, G. 1972. Un esempio di torbiditi di conoide sottomarina esterna: le arenarie di S. Salvatore (Formazione di Bobbio, Miocene) nell'Appennino di Piacenza. *Mem. Acc. Sc. Torino, Cl. Sc. Mat. Fis. Nat., Serie* 4 **16**, 1–40.

Petit, J. P. & Laville, E. 1987. Morphology and microstructure of hydroplastic slickenslides in sandstone. In: *Deformation of Sediments and Sedimentary Rocks* (edited by Jones, M. E. & Preston, R. M. F.). *Spec. Publs geol. Soc. Lond.* **29**, 107–122.

Platt, J. P. 1986. Dynamics of orogenic wedges and the uplift of high-pressure metamorphic rocks. *Bull. geol. Soc. Am.* **97**, 1037–1053.

Platt, J. P., Leggett, J. K. & Alam, S. 1988. Slip vectors and fault mechanics in the Makran Accretionary Wedge, Southwest Pakistan. *J. geophys. Res.* **93**, 7955–7973.

Plesi, G. 1974. L'Unità di Canetolo nella struttura di Bobbio (Val Trebbia), Montegroppo (Val Gotra) et lungo la trasversale Cinque Terre-Pracchiola. *Atti Soc. Tosc. Sc. Nat., Mem., Serie A* **81**, 121–151.

Ramsay, J. G. 1980. The crack–seal mechanism of rock deformation. *Nature* **284**, 135–139.

Ramsay, J. G. & Huber, M. 1983. *The Techniques of Modern Structural Geology, Vol.* 1: *Strain Analysis*. Academic Press, London.

Reutter, K. J. & Schlüter, H. U. 1968. La struttura delle arenarie di M. Modino-M. Cervarola nella zona di Bobbio (Piacenza) e nell'Appennino modenese. *L'Ateneo Parmense-Acta Naturalia* **4**, 1–23.

Ricci Lucchi, F. 1986. The Oligocene to Recent foreland basins of the Northern Apennines. In: *Foreland Basins* (edited by Allen, P. A. & Homewood, P.). *Spec. Publs Int. Ass. Sediment.* **8**, 105–139.

Ricci Lucchi, F. 1987. Semi-allochthonous sedimentation in the Apenninic thrust belt. *Sediment. Geol.* **50**, 119–134.

Rutter, E. H., Maddock, R. H., Hall, S. H. & White, S. H. 1986. Comparative microstructures of natural and experimentally produced clay-bearing fault gouges. *Pure & Appl. Geophys.* **124**, 3–30.

Shi, Y. & Wang, C. 1988. Generation of high pore pressures in accretionary prisms: inferences from the Barbados subduction complex. *J. geophys. Res.* **93**, 8893–8910.

Tchalenko, J. S. 1968. The evolution of kink-bands and the development of compression textures in sheared clays. *Tectonophysics* **6**, 159–174.

Tchalenko, J. S. 1970. Similarities between shear zones of different magnitudes. *Bull. geol. Soc. Am.* **81**, 1625–1640.

Treves, B. 1984. Orogenic belts as accretionary prisms: the example of the Northern Apennines. *Ofioliti* **9**, 577–618.

Von Huene, R. 1985. Direct measurement of pore fluid pressure, Leg 84, Guatemala and Costa Rica. *Init. Reps DSDP, Washington* (U.S. Govt Printing Office), **LXXXIV**, 767–772.

Von Huene, R. & Lee, H. 1982. The possible significance of pore fluid pressures in subduction zones. In: *Studies in Continental Margin Geology* (edited by Watkins, J. S. & Drake, C. L.). *Mem. Am. Ass. Petrol. Geol.* **34**, 781–791.

Vrolijk, P., Myers, G. & Moore, J. C. 1988. Warm fluid migration along tectonic melanges in the Kodiak Accretionary Complex, Alaska. *J. geophys. Res.* **93**, 10,313–10,324.

Will, T. M. & Wilson, C. J. L. 1989. Experimentally produced slickenside lineations in pyrophyllitic clay. *J. Struct. Geol.* **11**, 657–667.